ACS Macro Letters

Letter

pubs.acs.org/macroletters

Polymerization-Amplified Optical DNA Detection on Porous Silicon Templates

Dirk Holthausen,[†] Roshan B. Vasani,[‡] Steven J. P. McInnes,[‡] Amanda V. Ellis,[†] and Nicolas H. Voelcker*[,‡]

[†]School of Chemical and Physical Sciences, Flinders University, Bedford Park, South Australia 5042, Australia

[‡]Mawson Institute, University of South Australia, Mawson Lakes, South Australia 5095, Australia

Supporting Information

ABSTRACT: A porous silicon-based optical DNA sensor is described herein, which enables rapid DNA detection. The DNA sensor relies on the specificity of the DNA base pairing in conjunction with an interferometric optical signal amplification step based on polymer formation within the porous silicon layer to detect the DNA targets in a highly selective fashion. We demonstrate that it is possible to discriminate between DNA strands exhibiting even a single nucleotide mismatch using this sensor.

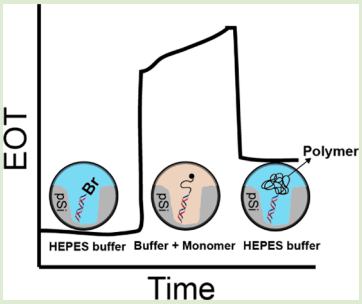

DNA sensing has a variety of applications, especially in medical science, forensics, ecology, and biotechnology.[1−4] Currently, the methods used for detection of DNA rely on either DNA labeling or DNA amplification using polymerase chain reaction. While these methods are widely accepted, they are also time-consuming and require the use of very sophisticated and expensive instrumentation. As a result, over the last few decades a variety of studies have focused on the development of DNA sensors that would enable the detection of minute quantities of DNA over shorter time frames.[2,5−9] Additionally, the ability to selectively discriminate between even single nucleotide mismatches is desirable for the identification of point mutations and diseases.

A recent development in the field of DNA sensing involves the formation of polymers by means of controlled radical polymerization methods such as atom transfer radical polymerization (ATRP)[10] or reversible addition−fragmentation chain transfer polymerization (RAFT)[11] to amplify the signal of the target DNA strand binding to a capture strand immobilized on surfaces. The use of controlled radical polymerization instead of conventional polymerization methods is advantageous as the polymer growth from surfaces has been shown to be linear with respect to time,[12] which may facilitate quantitative detection.

Qian et al. have used an ATRP version that is less sensitive to oxygen called activators generated by electron transfer (AGET) to detect DNA binding.[13] In their work, DNA capture strands immobilized on gold surfaces were incubated with target DNA strands modified with an ATRP initiator. Following this, the surface was immersed in the monomer mix and allowed to polymerize. Quantitative detection of DNA hybridization was performed using ellipsometry.

Porous silicon (pSi) has been extensively studied for use as a biosensing platform owing to its unique optical properties. White light incident on the pSi layer reflects off the air/pSi and the pSi/Si interfaces and undergoes interference to produce Fabry-Pérot fringes that can be obtained using interferometric reflectance spectroscopy (IRS) and that, when Fourier transformed, afford an effective optical thickness (EOT) value.[14] Changes within the porous environment results in a change in the EOT, which can be easily measured in real-time.[15] An added advantage of pSi is that the high surface area affords higher sensitivity as compared to flat surfaces. However, previous studies with pSi platforms have shown that detection of hybridization of cDNA strands using IRS is difficult unless the signal is amplified by pore degradation.[16] This in turn has the disadvantage that the amplification mechanism prevents the reuse of the sensor.

Herein, we present a signal amplification mechanism using pSi as the optical sensing platform where polymer growth is detected in real-time. Our method uses IRS to monitor the polymer growth from ATRP initiator-modified target DNA strands hybridized to capture strands immobilized on the pSi surface. Scheme 1 shows the experimental procedure for the fabrication (Scheme 1A) and the DNA sequences used (Scheme 1B).

The pSi template was produced by electrochemical etching of highly phosphorus doped n-type silicon in 5% aqueous hydrofluoric acid in the presence of a nonionic surfactant (NCW1001). Analysis of the etched surfaces using scanning electron microscopy (SEM) revealed pores of roughly 88 ± 21 nm in diameter and a pore depth of approximately 2.3 μm (Figure S1A,B, see SI).

To minimize oxidation, the freshly etched samples were immediately hydrosilylated with undecylenic acid-*N*-hydrox-

Received: February 6, 2012
Accepted: June 27, 2012
Published: July 3, 2012

Scheme 1. Surface Functionality of the pSi Surface after Each Chemical Modification Step (A) and the 5′−3′ Nucleotide Sequence of the Different Types of ssDNA Used Here (B)

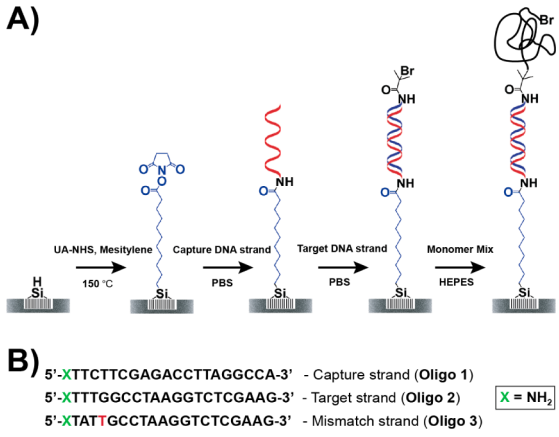

ysuccinimide ester (UA-NHS, 100 mM) in mesitylene for 16 h at 150 °C, as per our standard laboratory protocol.[17] The NHS-functionalized surfaces were then incubated in a phosphate buffered saline (PBS, pH 7.4) solution containing 20 μM 5′ amine-terminated ssDNA (Oligo 1), which was immobilized via an amide coupling reaction (Scheme 1A, red). The reaction was allowed to proceed overnight. Once the immobilization of ssDNA was complete, the unreacted NHS groups were quenched by incubating the surface with excess ethanolamine in PBS.

Attenuated total reflection−Fourier transform infrared spectroscopy (ATR-FTIR) analysis was used to examine the changes in the surface chemistry after each surface functionalization step, namely, (a) electrochemical anodization, (b) functionalization with UA-NHS, (c) immobilization of Oligo 1, and (d) ATRP with HEMA monomer (Figure 1A). The freshly

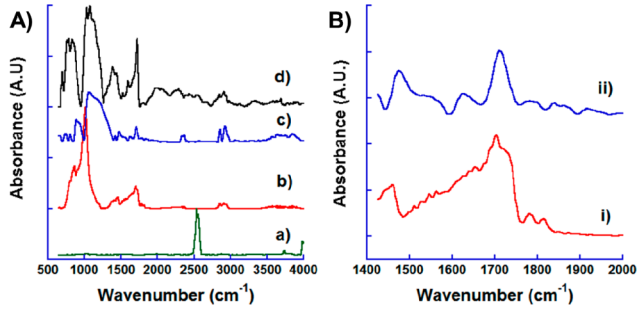

Figure 1. (A) ATR-FTIR spectra of the pSi surface after (a) electrochemical anodization, (b) hydrosilylation with UA-NHS, (c) immobilization of Oligo 1, and (d) ATRP with HEMA monomer; (B) Expanded region between 1400 and 2000 cm^{-1} of (i) the UA-NHS modified surface and (ii) the Oligo 1 modified surface.

etched pSi surface (Figure 1A-a) showed a strong band at 2100 cm^{-1}, which corresponds to the expected peak for Si−H vibrations.[18] After hydrosilylation of the pSi surface with the UA-NHS (Figure 1A-b), characteristic peaks corresponding to the C−H valence vibrations at approximately 2840 and 2910 cm^{-1} were observed, along with the disappearance of the Si−H vibrations. A strong peak at approximately 1070 cm^{-1} appeared that can be attributed to the formation of silicon dioxide on the surface.[19] Furthermore, peaks at around 1740, 1785, and 1820 cm^{-1} were also seen (Figure 1B) and were attributed to the stretching vibrations of carbonyls of the NHS ester.[20]

Following the incubation of the surface with Oligo 1 (prior to reacting the surface with ethanolamine; Figure 1A-c), the peaks at 1785 and 1820 cm^{-1} disappeared, which was indicative of the replacement of the NHS group. In addition, a shoulder peak at 1540 cm^{-1} and a weak peak at around 1640 cm^{-1} appeared that provided evidence for amide bond formation with the amine-terminated ssDNA. A broadening of the peak at 1100 cm^{-1} along with the appearance of a shoulder peak at 1230 cm^{-1} was also observed, which was attributed to the PO_2^- stretching vibration of the DNA backbone and the ring stretching modes of the base residues.[21] No change in the ATR-FTIR spectra was observed following the reaction of the surface with ethanolamine.

Before the hybridization step, the target DNA (Scheme 1B; Oligo 2) was modified with the ATRP initiator α-bromoisobutyryl bromide (BiBB). The initiator was coupled to the 5′ amine-terminus of the target ssDNA via a BiBB-NHS ester intermediate using a modified version of a procedure outlined in the literature.[22] To hybridize the surface-immobilized capture DNA strand and initiator-modified target DNA, the prepared pSi sample was incubated with target DNA (20 μM) in 4-(2-hydroxyethyl)piperazine-1-ethanesulfonic acid (HEPES) buffer for 1 h. For all experiments described below, the same concentrations of capture and target strands were used. The AGET-ATRP reaction was carried out in a custom-built flow cell to allow for both the buffer and monomer solutions to be pumped over the surface. The flow cell was transparent to facilitate monitoring of the polymerization via IRS. The pSi sample was placed in the flow cell and HEPES buffer was flowed through the cell using a syringe pump. The pSi film showed the typical interference fringes of a Fabry-Pérot layer (Figure 2A) from which the EOT was obtained via Fourier transformaton. Buffer was flowed over the pSi surface for approximately 15 min to obtain a baseline EOT response. Following this, a monomer mixture consisting of copper(II)

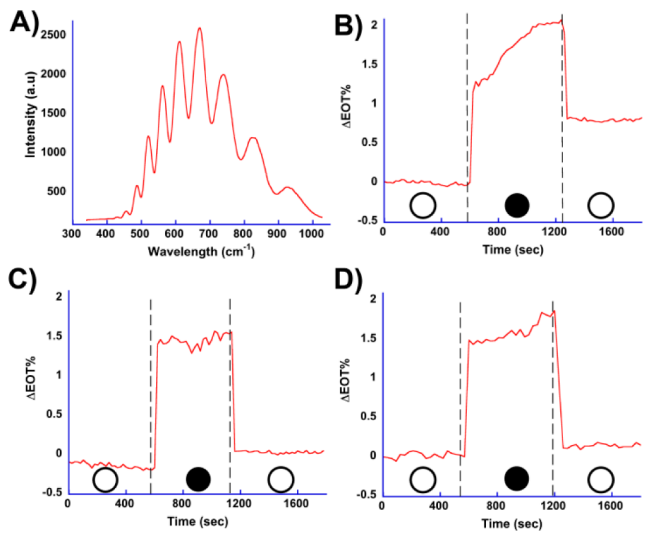

Figure 2. (A) Typical Fabry-Pérot fringes observed on *n*-type pSi; IRS spectra of (B) a DNA sensor incubated with Oligo 2, (C) DNA sensor without target ssDNA (control), and (D) a sensor incubated with Oligo 3; The open circle (○) indicates incubation periods with HEPES buffer and the filled circle (●) indicates incubation periods with the monomer mixture.

dx.doi.org/10.1021/mz300064k | *ACS Macro Lett.* 2012, 1, 919−921

bromide, 2,2′-bipyridine, ascorbic-acid, and a 2:1 Tris buffer/2-hydroxyethyl methacrylate (HEMA) solution was flowed over the surface for 10 min. The surface was then washed with 20% ethanol in PBS followed by excess of HEPES buffer to remove unbound polymer. Figure 1A-d shows the ATR spectrum of the surface post polymerization. A strong IR peak at around 1740 cm^{-1} was observed that was attributed to the carbonyl stretching vibration of the polymer and also a broad peak between 3000 and 3500 cm^{-1}, characteristic of the stretching vibrations of the hydroxyl groups on the polymer.[10] The peaks confirm the formation of polymer and, hence, the success of the AGET ATRP reaction in the porous layer.

Figure 2 shows typical IRS results obtained from the DNA sensing experiments. When the Oligo 1 modified surface was hybridized to the initiator-modified cDNA (Oligo 2), an initial sharp increase in EOT was observed on flowing the HEMA monomer mixture over the pSi surface, followed by a more gradual increase (Figure 2B). The initial increase was due to the difference in refractive index of the HEMA monomer mixture compared to the HEPES buffer. The following gradual increase was attributed to the formation of polymer within the pores. After washing the pSi surface with HEPES buffer to remove any unbound polymer and comparing the final EOT to the initial baseline in HEPES buffer, a definitive increase in the EOT of 0.80 ± 0.10% (n = 3) was observed, which was reproducible throughout the experiments. In contrast to this, control experiments (Figure 2C) where the surface was not incubated with a target strand showed a much lower increase in EOT of 0.16 ± 0.04% (n = 3). This slight increase in EOT could be attributed to the presence of adsorbed polymer formed via an initiator-less pathway that is typical for aqueous AGET ATRP systems, as previously reported.[23] However, the clear and reproducible difference in the EOT signal between the control samples and the sample containing target DNA allows the identification of DNA hybridization on pSi surfaces.

Experiments to test the selectivity of the sensor were also performed by using a ssDNA strand featuring a single base mismatch (Scheme 1B; Oligo 3). Similar to the procedure described above, the initiator-modified Oligo 3 strand was incubated with a surface functionalized with the capture strand Oligo 1 and then placed into the flow cell setup. On flowing the monomer mixture over the surface, no significant increase in EOT (0.11 ± 0.01%; n = 3) was observed, as in the case of the control runs (Figure 2D), demonstrating the capacity for mismatch detection using this sensor. Experiments were also conducted to confirm that the hybridization event could not be directly detected on the pSi surface without a signal amplification step. To do so, the DNA sensor surface functionalized with Oligo 1 was incubated with Oligo 2 while monitoring with IRS (data not shown). No significant change in the EOT was observed in this case, demonstrating that the change in refractive index as a result of cDNA hybridization into the porous layer does not permit detection by IRS on a single layer pSi film.

It should also be noted that it is possible to design a capture strand that is shorter than the target leaving a sticky end, which can then be hybridized to a short cDNA strand modified with the ATRP initiator. This concept has been previously demonstrated by Lou et al.[10]

In summary, we have successfully prepared and demonstrated an optically transduced AGET-ATRP amplified DNA biosensor on a pSi film. The sensor allowed for rapid detection of target DNA. The sensor exhibited selectivity for the target strand with the ability to discriminate a single base-pair mismatch. This selectivity could prove useful for the detection of point mutations as disease markers. This sensor might provide a cheap and quick alternative for DNA sensing to the current commercially available options.

■ ASSOCIATED CONTENT

Ⓢ Supporting Information

Detailed experimental procedures and SEM images of the porous silicon surface. This material is available free of charge via the Internet at http://pubs.acs.org.

■ AUTHOR INFORMATION

Corresponding Author

*E-mail: nico.voelcker@unisa.edu.au.

Notes

The authors declare no competing financial interest.

■ ACKNOWLEDGMENTS

The authors would like to thank the Australian Research Council for financial support.

■ REFERENCES

(1) Arzum, E. *Talanta* **2007**, *74*, 318−325.
(2) Cosnier, S.; Mailley, P. *Analyst* **2008**, *133*, 984−991.
(3) Joseph, W. *Anal. Chim. Acta* **2002**, *469*, 63−71.
(4) Fan, X.; White, I. M.; Shopova, S. I.; Zhu, H.; Suter, J. D.; Sun, Y. *Anal. Chim. Acta* **2008**, *620*, 8−26.
(5) Drummond, T. G.; Hill, M. G.; Barton, J. K. *Nat. Biotechnol.* **2003**, *21*, 1192−1199.
(6) Chen, X.-J.; Sanchez-Gaytan, B. L.; Qian, Z.; Park, S.-J. *Wiley Interdiscip. Rev.: Nanomed. Nanobiotechnol.* **2012**, *4*, 273−290.
(7) Tao, Y.; Lin, Y.; Huang, Z.; Ren, J.; Qu, X. *Analyst* **2012**, *137*, 2588−2592.
(8) Yang, S.; Liu, Y.; Tan, H.; Wu, C.; Wu, Z.; Shen, G.; Yu, R. *Chem. Commun.* **2012**, *48*, 2861−2863.
(9) Zanoli, L.; D'Agata, R.; Spoto, G. *Anal. Bioanal. Chem.* **2012**, *402*, 1759−1771.
(10) Lou, X.; Lewis, M. S.; Gorman, C. B.; He, L. *Anal. Chem.* **2005**, *77*, 4698−4705.
(11) He, P.; Zheng, W.; Tucker, E. Z.; Gorman, C. B.; He, L. *Anal. Chem.* **2008**, *80*, 3633−3639.
(12) Edmondson, S.; Osborne, V. L.; Huck, W. T. S. *Chem. Soc. Rev.* **2004**, *33*, 14−22.
(13) Qian, H.; He, L. *Anal. Chem.* **2009**, *81*, 4536−4542.
(14) Lin, V. S.-Y.; Motesharei, K.; Dancil, K.-P. S.; Sailor, M. J.; Ghadiri, M. R. *Science* **1997**, *278*, 840−843.
(15) Vasani, R. B.; McInnes, S. J. P.; Cole, M. A.; Jani, A. M. M.; Ellis, A. V.; Voelcker, N. H. *Langmuir* **2011**, *27*, 7843−7853.
(16) Voelcker, N. H.; Alfonso, I.; Ghadiri, M. R. *ChemBioChem* **2008**, *9*, 1776−1786.
(17) Wojtyk, J. T. C.; Morin, K. A.; Boukherroub, R.; Wayner, D. D. M. *Langmuir* **2002**, *18*, 6081−6087.
(18) Bisi, O.; Ossicini, S.; Pavesi, L. *Surf. Sci. Rep.* **2000**, *38*, 1−126.
(19) Mawhinney, D. B.; Glass, J. A.; Yates, J. T. *J. Phys. Chem. B* **1997**, *101*, 1202−1206.
(20) Pei, J.; Tang, Y.; Xu, N.; Lu, W.; Xiao, S.; Liu, J. *Sci. China Chem.* **2011**, *54*, 526−535.
(21) Ushizawa, K.; Sato, Y.; Mitsumori, T.; Machinami, T.; Ueda, T.; Ando, T. *Chem. Phys. Lett.* **2002**, *351*, 105−108.
(22) Lou, X.; He, L. *Langmuir* **2006**, *22*, 2640−2646.
(23) Hermant, M. C.; Kaya, Z. N.; Vasani, R.; Lewis, D. A. *Abstr. Pap. Am. Chem. Soc.* **2011**, 241.